

## **BROADBAND SHORTED SECTORAL MICROSTRIP ANTENNA**

**A. A. Deshmukh**

DJSCOE

Vile-Parle (W), Mumbai 400 056, India

**K. P. Ray**

SAMEER, I.I.T. Campus

Powai, Mumbai 400 076, India

**Abstract**—The broadband microstrip antenna is realized by cutting the slot inside the patch. The slot introduces a resonant mode near the fundamental resonance frequency of the antenna and realizes broadband response. The compact variations of circular microstrip antenna are realized by placing the shorting posts along the zero field line at the fundamental mode. These shorted antennas have narrower bandwidth. In this paper, a compact half U-slot cut shorted sectoral microstrip antenna is proposed. The detailed analysis has been carried out to study the effect of the slot on various modes of the sectoral patch. It has been observed that the half U-slot does not introduce any additional mode, but reduces the resonance frequency of the higher order mode of the shorted sectoral patch and along with its fundamental mode realizes broader bandwidth. The bandwidth of more than 700 MHz, at the center frequency of approximately 2700 MHz, has been realized.

### **1. INTRODUCTION**

The broadband microstrip antenna (MSA) is realized by cutting U-slot, V-slot and a pair of rectangular slots inside the patch [1–8]. It is assumed that the slot introduces an additional mode near the fundamental mode of the MSA (i.e.,  $TM_{10}$  for rectangular MSA,  $TM_{11}$  for circular MSA and  $TM_{10}$  for equilateral triangular MSA) and thus realizes broadband response. While designing these slot cut MSAs

---

*Received 2 January 2011, Accepted 21 February 2011, Scheduled 1 March 2011*

Corresponding author: Amit A. Deshmukh (amitdeshmukh76@yahoo.com).

for a given frequency range, the slot length is taken to be nearly half wavelength when cutting inside the patch or quarter wavelength when cutting on the edges of the patch. However, it was observed that the surface currents encircle over a finite length towards the shorted end of the slot, which adds to the additional length [9]. Thus, after adding this correction length, the slot length for the required frequency is calculated. This correction length was found to be 10% of the slot length [9]. By using the symmetry of slot cut MSAs across the feed point axis, a compact and broadband MSAs by cutting a half U-slot, half V-slot or a single slot has been realized [8, 10–12]. These compact MSAs realize 50% reduction in the patch size with nearly the same BW. When the loop formed (due to the coupling between patch mode and mode introduced by the slot) in the input impedance locus is larger (i.e., it does not lie inside  $VSWR = 2$  circle), then a dual band response is realized using these slot cut MSAs [13–16]. While designing these dual and broad band MSAs for a given frequency band, simpler half and quarter wavelength approximations of slot length do not give closer results for various slot lengths and different slot positions inside the patch. Also, a formulation of resonant length in U-slot or half U-slot cut MSAs is not reported [17]. The frequency response in dual band U-slot and pair of rectangular slots cut inside the circular MSA (CMSA), for different slot dimensions, was studied over wide frequency range. It was observed that neither U-slot nor rectangular slots introduce any additional mode, but they reduce the higher order  $TM_{21}$  mode resonance frequency of the circular patch and thus, along with fundamental  $TM_{11}$  mode, realizes dual band response [18]. The resonant length formulation for slot mode frequency (modified  $TM_{21}$  mode) has been proposed [18].

The  $90^\circ$  sectoral MSA is a compact variation of CMSA and is realized by placing the shorting plate along the zero field line of CMSA at its fundamental  $TM_{11}$  mode [19]. In this paper, a broadband half U-slot cut  $90^\circ$  sectoral MSA is proposed. The surface current distributions at various resonant modes of the half U-slot cut  $90^\circ$  sectoral MSA over large frequency range have been studied. It is observed that the half U-slot does not introduce any mode but reduces the higher order  $TM_{31}$  mode resonance frequency of the shorted sectoral MSA. This mode with reduced resonance frequency, along with the fundamental  $TM_{11}$  mode, yields broadband response. This sectoral MSA gives a bandwidth (BW) of more than 700 MHz ( $> 25\%$ ) at around 2700 MHz. The radiation pattern at shorted  $TM_{31}$  mode in sectoral MSA shows higher cross-polarization levels. Also, it shows variation in the directions of  $E$  and  $H$ -planes as compared to the radiation pattern at shorted  $TM_{11}$  mode. However, since the half U-

slot alters  $s$  of the principle planes. To optimize for the gain and to realize larger BW, the sectoral MSA is analyzed using the air substrate having substrate thickness of  $\leq 1.2$  cm ( $0.1\lambda_0$ ). In the present configuration, substrate thickness of 0.8 cm is used. The antenna is fed using the SMA panel type connector having inner wire diameter of 0.12 cm. The sectoral MSA was first analyzed using IE3D software followed by experimental verification [20]. The measurements were carried out using HP vector network analyzer. To realize the effect of infinite ground plane, in the measurements a larger ground plane size of  $30 \times 30$  cm is taken. Further, the antenna response is also validated on smaller ground plane of size  $10 \times 10$  cm, which could be used in its practical applications. The radiation patterns were measured in minimum reflection surroundings with the required minimum distance between the reference antenna and the antenna under test [21].

## 2. FUNDAMENTAL AND HIGHER ORDER MODES OF CMSA

The resonance frequency of the CMSA is given by Equation (1) [19].

$$f_{nm} = K_{nm}c/2\pi r_e(\epsilon_r)^{1/2} \quad (1)$$

where,  $f_{nm}$  = resonance frequency of  $TM_{nm}$  mode,  $c$  = velocity of light =  $3 \times 10^8$  (m/s),  $K_{nm}$  is the  $m$ th zero of the derivative of the Bessel function of  $n$ th order, which is = 1.84118 ( $TM_{11}$ ), 3.05424 ( $TM_{21}$ ), 3.83171 ( $TM_{02}$ ), 4.20119 ( $TM_{31}$ ), 5.317 ( $TM_{41}$ ), 5.3314 ( $TM_{12}$ ),  $r_e$  = effective radius of the patch after accounting for the fringing fields around the periphery of the patch.

For CMSA with patch radius ( $r$ ) equal to 3.2 cm and with substrate thickness ( $h$ ) of 0.8 cm, as shown in Figs. 1(a), (b), the resonance frequencies of various modes calculated using Eq. (1) are  $f_{TM_{11}} = 2345$  MHz,  $f_{TM_{21}} = 3892$  MHz,  $f_{TM_{02}} = 4882$  MHz,  $f_{TM_{31}} = 5353$  MHz and  $f_{TM_{41}} = 6345$  MHz. This CMSA has been simulated using IE3D software, and the resonance curve for the same is shown in Fig. 1(c). The first peak, in the resonance curve, corresponds to  $TM_{11}$  mode at frequency of 2224 MHz. In this mode, the patch surface currents and the peripheral voltage distribution show one half wavelength variations along the patch diameter and a wavelength variation around the perimeter of the patch, as shown in Fig. 1(d). The second peak corresponds to  $TM_{21}$  mode (3758 MHz) at which peripheral voltage shows two wavelength variations around the perimeter of the CMSA and one half wavelength variations along its diameter as shown in Fig. 1(e). The third peak corresponds to  $TM_{31}$  mode (5331 MHz) at which the peripheral voltage shows

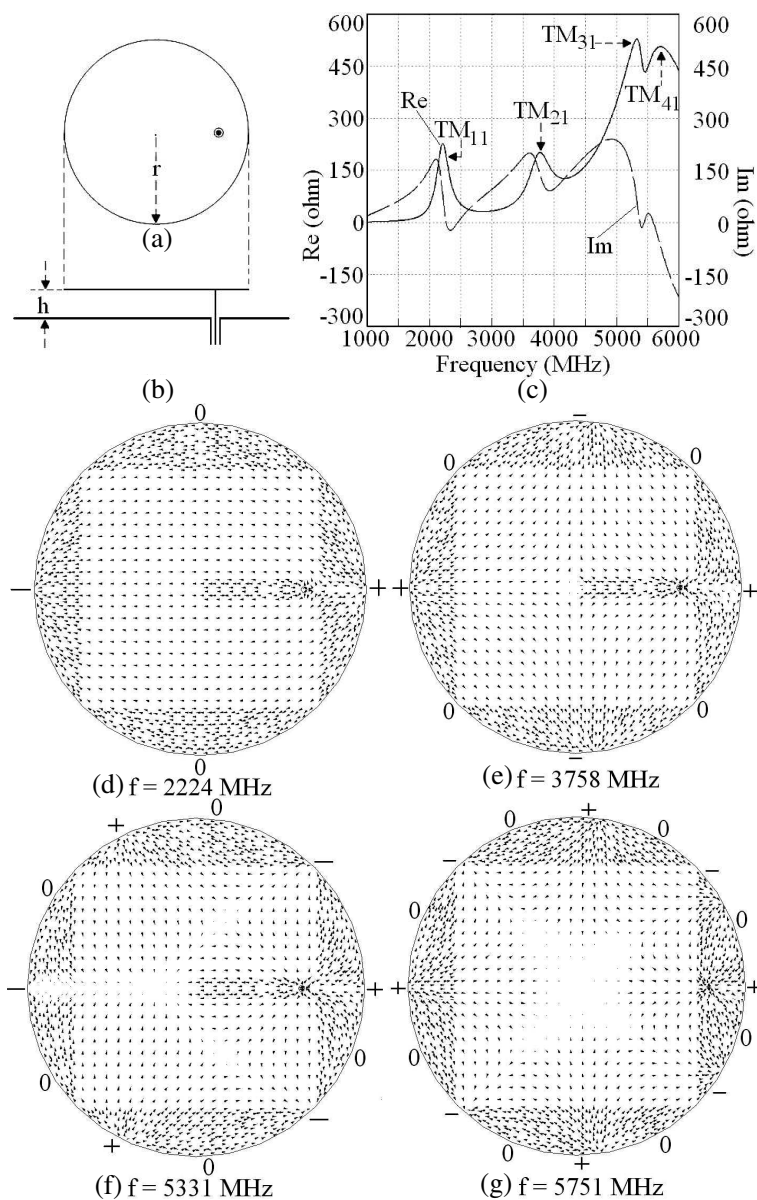


**Figure 1.** (a) Top and (b) side views of CMSA and its (c) simulated resonance curve plot and its surface current and voltage distributions at (d)  $TM_{11}$ , (e)  $TM_{21}$ , (f)  $TM_{31}$ , (g)  $TM_{41}$  modes.

three wavelength variations along the perimeter of the patch and one half wavelength variations along its diameter as shown in Fig. 1(f). The last peak corresponds to  $TM_{41}$  mode (5751 MHz). At this frequency, peripheral voltage shows four wavelength variations around the perimeter of the CMSA and one half wavelength variations along its diameter as shown in Fig. 1(g).

The CMSA in its  $TM_{11}$  mode has the simulated BW of 234 MHz (8.9%). The compact shorted plate  $90^\circ$  sectoral MSA is realized by placing the shorting plate along the zero field line of  $TM_{11}$  mode and further by using only half of the patch as shown in Figs. 2(a), (b). This compact MSA realizes 75% reduction in the patch area with nearly the same resonance frequency [19]. The resonance curve plot for shorted sectoral MSA is shown in Fig. 2(c). The first peak corresponds to  $TM_{11}$  mode at 1960 MHz. Since the CMSA is shorted in the center, in shorted sectoral MSA, the  $TM_{21}$  and  $TM_{02}$  modes do not get excited as they have maximum field in the center of the patch. The  $TM_{31}$  mode has zero fields in the center of the patch and hence along with  $TM_{11}$  mode, the  $TM_{31}$  mode (4560 MHz) is present in shorted sectoral MSA as seen in its resonance curve plot. The surface current and voltage distribution plots at shorted  $TM_{11}$  and  $TM_{31}$  modes are shown in Figs. 2(d), (e). To increase the BW of shorted  $90^\circ$  sectoral MSA, a half U-slot is cut inside the patch as discussed in the following section.

### 3. BROADBAND $90^\circ$ SECTORAL HALF U-SLOT CUT MSA

A half U-slot cut shorted  $90^\circ$  sectoral MSA is shown in Fig. 3(a). To optimize for broader BW a parametric study by varying half U-slot dimensions were carried out. The resonance curve plots for varying half U-slot lengths ( $L_h$  and  $L_v$ ) are shown in Figs. 3(b), (c). Initially  $L_h$  is increased as shown in Fig. 3(b). The  $L_h$  is orthogonal to the surface currents at  $TM_{31}$  mode whereas it is parallel to surface currents at  $TM_{11}$  mode. Hence the  $TM_{31}$  frequency reduces and  $TM_{11}$  frequency remains almost unchanged. Further when both  $L_h$  and  $L_v$  are increased then  $TM_{31}$  as well as  $TM_{11}$  frequency reduces. The length  $L_v$  is orthogonal to surface currents at  $TM_{11}$  mode and therefore its frequency reduces. Thus with increase in the slot length the  $TM_{31}$  frequency comes closer to  $TM_{11}$  frequency and the broadband response is realized when the loop, which gets formed because of the mutual coupling between these two modes, lies inside the  $VSWR = 2$  circle. To realize this,  $L_v$  and  $L_h$  are optimized. In the optimized configuration,  $L_h$  and  $L_v$  are 2.4 and 1.0 cm, respectively. The input impedance and VSWR plots are shown in Fig. 4(a). The simulated BW is 740 MHz

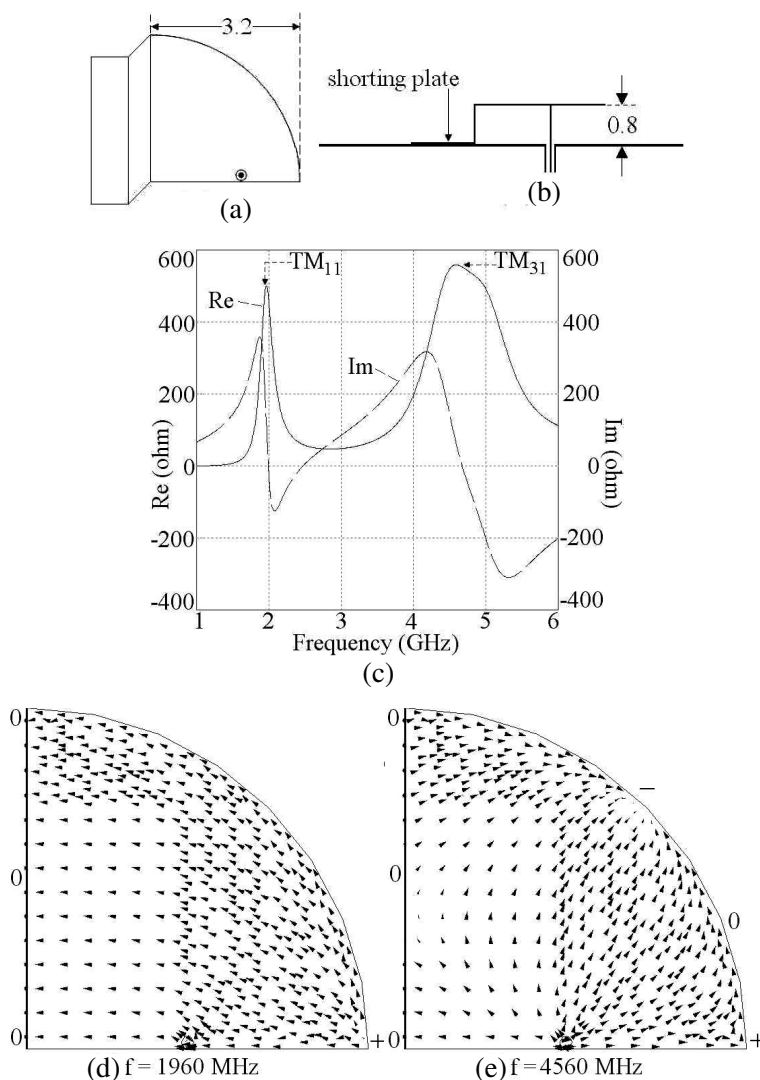


**Figure 2.** (a) Top and (b) side views of shorted plate 90° sectoral MSA, its (c) resonance curve plot and its surface current distributions at shorted (d) TM<sub>11</sub> and (e) TM<sub>31</sub> modes.

(28%). The broadband response has been experimentally verified. The measured BW is 768 MHz (29%). The variation in the measured and simulated results is due to the experimental errors. The picture of the fabricated prototype is shown in Fig. 4(b).

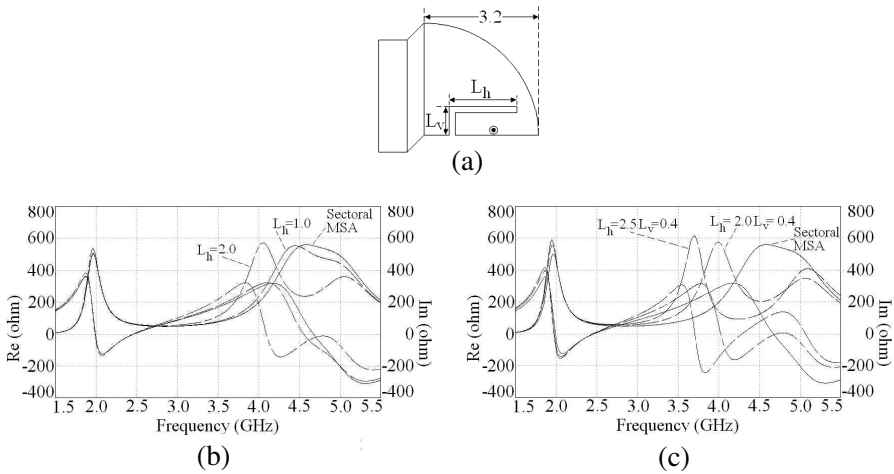


**Figure 3.** (a) Half U-slot cut shorted plate 90° sectoral MSA and its (b), (c) resonance curve plots for different U-slot lengths.

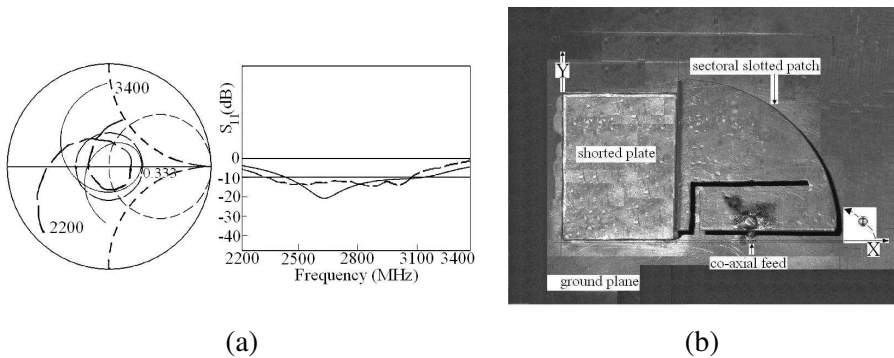


**Figure 4.** (a) Input impedance and return loss plots (—) simulated, (---) measured and (b) photograph of fabricated prototype of half U-slot cut 90° sectoral MSA.

The simulated surface current distribution over the BW is shown in Figs. 5(a)–(c). At the lower frequency end of the BW, shorted  $TM_{11}$  mode is dominant whereas towards the higher frequencies end of the BW, the shorted  $TM_{31}$  mode is dominant. This distribution is similar to that of  $TM_{31}$  mode distribution as shown in Fig. 2(e). The radiation pattern and measured gain over the BW are shown in Figs. 6(a)–(d). The  $E$  and  $H$ -planes are aligned along  $\Phi = 0^\circ$  and  $90^\circ$ , respectively over the entire BW. Due to the shorted patch and electrically thicker air substrate, the radiation pattern shows maximum radiation towards

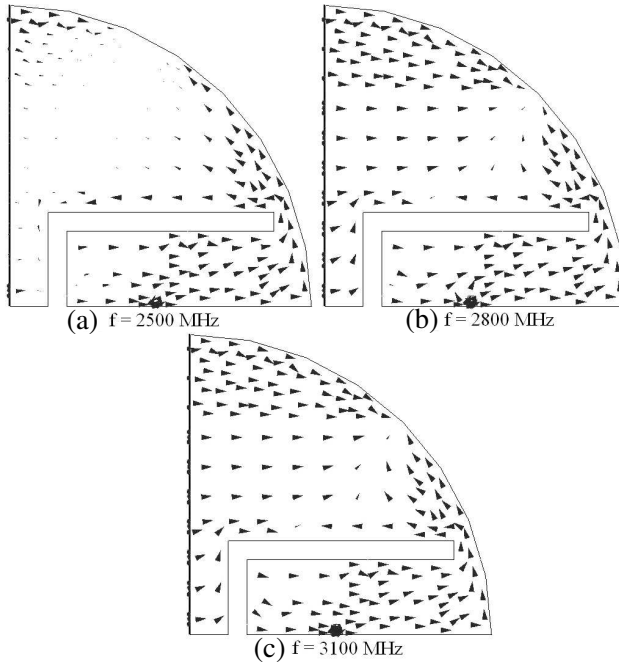


**Figure 5.** (a)–(c) Surface current distributions at three frequencies over the BW for half U-slot cut  $90^\circ$  sectoral MSA.

$+90^\circ$  and  $-90^\circ$  directions with a broadside level at 3 dB down. The cross-polarization levels are less than 7 dB as compared to the co-polar levels. As the  $TM_{31}$  mode is dominant at the higher frequencies end of the BW, a higher cross-polarization level is present. In the entire BW range, due to the air substrate, the radiation efficiency is greater than 95%. The antenna gain is more than 4 dBi over the entire VSWR BW with a peak gain of nearly 6.8 dBi towards the higher frequencies end of the BW. The radiation patterns were measured using larger ground plane size, thus they do not show any back lobe radiation. The measurement was also carried out using  $10 \times 10$  cm ground plane size. This reduced ground plane showed back lobe radiation 7 dB down as compared to the main lobe radiation with similar input impedance characteristics.

For the substrate thickness of 0.8 cm, the simulated BW of the CMSA is 234 MHz (8.9%) whereas the U-slot cut CMSA has the simulated BW of 464 MHz (19.7%). The shorted plate  $90^\circ$  sectoral MSA gives the simulated BW of 359 MHz (14.2%). Thus the proposed compact configuration gives more BW as compared to the conventional CMSA, U-slot cut CMSA and the shorted plate  $90^\circ$  sectoral suspended



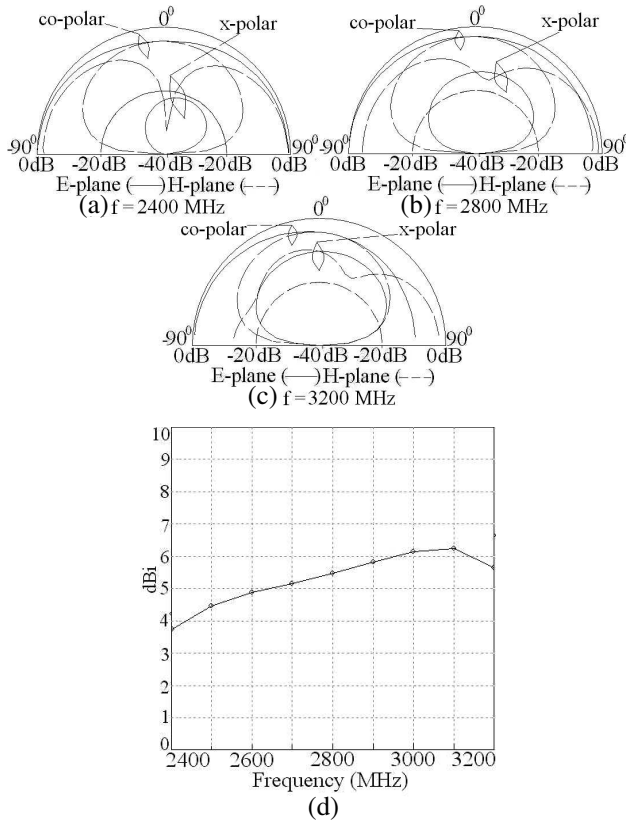


**Figure 6.** (a)–(c) Radiation patterns at three frequencies and (d) gain variation over BW for half U-slot cut  $90^\circ$  sectoral MSA.

MSA. The larger BW is due to the use of electrically thicker substrate, a shorting plate and a half U-slot which controls the  $TM_{31}$  mode frequency with respect to  $TM_{11}$  mode frequency. Although, the cross-polarization levels are higher, they are useful in applications of multipath propagation environment wherein, these compact antennas will lead to smaller signal loss.

#### 4. CONCLUSION

The voltage and current distributions at higher order modes in CMSA are discussed. In its compact shorted  $90^\circ$  sectoral MSA, the  $TM_{11}$  and  $TM_{31}$  modes are present. A broadband  $90^\circ$  sectoral half U-slot cut MSA is proposed. The frequency response over the wide

frequency range for varying half U-slot dimensions has been studied. It is observed that the half U-slot does not introduce any mode but alters the higher order  $TM_{31}$  mode resonance frequency of the patch. This modified higher order mode, along with the fundamental  $TM_{11}$  mode, yields broader BW. The proposed  $90^\circ$  sectoral half U-slot cut MSA gives the BW of more 700 MHz at around 2700 MHz. The half U-slot alters the directions of surface currents on the patch at  $TM_{31}$  mode and hence the radiation pattern shows no variation in the direction of principle planes over the BW. This antenna gives 75% reduction in the size of the patch with nearly four times the BW as compared to the CMSA and more than 1.5 times the BW as compared to that of the U-slot cut CMSA. A good agreement is obtained between the measured and simulated input impedance plots, gains and the radiation patterns.

## REFERENCES

1. Wong, K. L., *Compact and Broadband Microstrip Antennas*, John Wiley & Sons, Inc., New York, USA, 2002.
2. Huynh, T. and K. F. Lee, "Single-layer single-patch wideband microstrip antenna," *Electronics Letters*, Vol. 31, No. 16, 1310–1312, Aug. 1995.
3. Wong, K. L. and W. H. Hsu, "A broadband rectangular patch antenna with a pair of wide slits," *IEEE Transactions on Antennas & Propagation*, Vol. 49, 1345–1347, Sep. 2001.
4. Guo, Y. X., K. M. Luk, K. F. Lee, and Y. L. Chow, "Double U-slot rectangular patch antenna," *Electronics Letters*, Vol. 34, 1805–1806, 1998.
5. Lee, K. F., K. M. Luk, K. F. Tong, S. M. Shum, T. Huynh, and R. Q. Lee, "Experimental and simulation studies of the coaxially fed U-slot rectangular patch antenna," *IEE Proceedings — Microwave Antennas and Propagation*, Vol. 144, No. 5, 354–358, 1997.
6. Tong, K. F., K. M. Luk, K. F. Lee, and R. Q. Lee, "A broadband U-slot rectangular patch antenna on a microwave substrate," *IEEE Transactions on Antennas & Propagation*, Vol. 48, No. 6, 954–960, 2000.
7. Weigand, S., G. H. Huff, K. H. Pan, and J. T. Bernhard, "Analysis and design of broadband single layer rectangular U-slot microstrip patch antenna," *IEEE Transactions on Antennas & Propagation*, Vol. 51, No. 3, 457–468, 2003.
8. Deshmukh, A. A. and G. Kumar, "Broadband and compact V-

- slot loaded RMSAs,” *Electronics Letters*, Vol. 42, No. 17, 951–952, Aug. 17, 2006.
9. Knorr, J. B. and J. Saenz, “End effect in a shorted slot,” *IEEE Trans. Microwave Theory & Techniques*, 579–580, Sep. 1973.
  10. Chair, R., K. F. Lee, C. L. Mak, K. M. Luk, and A. A. Kishk, “Miniature wideband half U-slot and half E patch antennas,” *IEEE Transactions on Antennas & Propagation*, Vol. 52, No. 8, 2645–2652, Aug. 2005.
  11. Deshmukh, A. A. and G. Kumar, “Compact broadband U-slot loaded rectangular microstrip antennas,” *Microwave & Optical Technology Letters*, Vol. 46, No. 6, 556–559, 2005.
  12. Deshmukh, A. A. and G. Kumar, “Compact broadband E-shaped microstrip antennas,” *Electronics Letters*, Vol. 41, No. 18, 989–990, 2005.
  13. Deshmukh, A. A. and G. Kumar, “Even mode multi-port network model for slotted dual band rectangular microstrip antennas,” *Microwave & Optical Technology Letters*, Vol. 48, No. 4, 798–804, 2006.
  14. Daniel, A. E. and R. K. Shevgaonkar, “Slot-loaded rectangular microstrip antenna for tunable dual-band operation,” *Microwave & Optical Technology Letters*, Vol. 44, No. 5, 441–444, Mar. 5, 2005.
  15. Lu, J. H., “Single feed dual frequency rectangular microstrip antenna with pair step slots,” *Electronics Letters*, Vol. 35, No. 5, 354–355, 1999.
  16. Boyle, K. R. and P. J. Massey, “Nine band antenna system for mobile phones,” *Electronics Letters*, Vol. 42, No. 5, 265–266, 2006.
  17. Lee, K. F., S. L. S. Yang, A. A. Kishk, and K. M. Luk, “The versatile U-slot patch,” *IEEE Antennas & Propagation Magazine*, Vol. 52, No. 1, 71–88, Feb. 2010.
  18. Deshmukh, A. A., K. P. Ray, T. Sonwadkar, S. Varawalla, and R. Kataria, “Formulation of resonance frequency for multi-band circular microstrip antennas,” *International Journal of Microwave and Optical Technology*, Vol. 5, No. 5, 248–256, Sep. 2010.
  19. Kumar, G. and K. P. Ray, *Broadband Microstrip Antennas*, Artech House, USA, 2003.
  20. IE3D 12.1, Zeland Software, Freemont, USA, 2004.
  21. Balanis, C. A., *Antenna Theory: Analysis and Design*, 2nd edition, John Wiley & Sons Ltd., 1996.